CSAWAC 44 (8) 909-1084 (2016) · Vol. 44 · No. 8 · August 2016

CLEAN
Soil Air Water

Renewables

Sustainability

Environmental Monitoring

8 | 2016

www.clean-journal.com

WILEY

CLEAN
Soil Air Water

Mu. Naushad[1]
Mohammad Rizwan Khan[1]
Zeid Abdullah ALOthman[1]
Ala'a H. Al-Muhtaseb[2]
Md. Rabiul Awual[3]
Ayoub Abdullah Alqadami[1]

[1]Department of Chemistry, College of Science, King Saud University, Riyadh, Saudi Arabia
[2]Faculty of Engineering, Department of Petroleum and Chemical Engineering, Sultan Qaboos University, Muscat, Oman
[3]Actinide Chemistry Group, Material Sciences and Research Centre, Japan Atomic Energy Agency (SPring–8), Hyogo, Japan

Research Article

Water Purification Using Cost Effective Material Prepared from Agricultural Waste: Kinetics, Isotherms, and Thermodynamic Studies

The usage of agricultural waste-based bio-adsorbents for the removal of environmental pollutants from water is gaining extensive attention. In this paper, carrot residue (CR) (*Daucus carota* L.) was used for the production of activated carbon (AC) via chemical activation with HNO_3. CR derived activated carbon (CAC) was characterized by various analytical techniques. The Brunauer–Emmett–Teller surface area was found to be 17.76 $m^2\,g^{-1}$. The efficacy of this AC in adsorbing BrO_3^- from water samples was studied at time, pH, temperature, and initial BrO_3^- concentrations by batch studies. The concentration of BrO_3^- was assessed by ultra-performance liquid chromatography-mass tandem spectrometry. A maximum adsorption capacity of 16.66 mg g^{-1} at 298 K was obtained from the Langmuir isotherms fit. The kinetic data followed closely the pseudo-first-order rate kinetic model. The thermodynamic study of BrO_3^- adsorption data showed that the adsorption was feasible, spontaneous, and endothermic in nature. The practical efficacy of CAC was performed for BrO_3^- removal from tap water as well as bottled water samples.

Keywords: Adsorption; Bromate; Carrot residue; UPLC-MS; Water samples

Received: January 11, 2016; *revised:* April 3, 2016; *accepted:* May 4, 2016

DOI: 10.1002/clen.201600027

1 Introduction

Basically, most of the industrial processes produce by-products that become waste materials and our environment is persistently exposed to pollution by these wastes such as heavy metals, phenols, pesticides, and bromate (BrO_3^-). Actually, BrO_3^- is a by-product which is developed at the time of disinfection of drinking water using O_3 or ClO_2^-. The World Health Organization, WHO, and European Commission, EC, have suggested the maximum level of contaminant for BrO_3^-, 10 $\mu g\,L^{-1}$ in drinking water [1]. In water samples, the formation of BrO_3^- takes place as [2]:

Using O_3:

$$O_3 + Br^- \rightarrow O_2 + OBr^-$$

$$O_3 + OBr^- \rightarrow 2\ O_2 + Br^-$$

$$2\ O_3 + OBr^- \rightarrow 2\ O_2 + BrO_3^-$$

Using ClO_2^-:

$$ClO_2^- + Br^- \rightarrow Cl_2O_3^- + OBr^-$$

$$3\ OBr^- \rightarrow 2\ Br^- + BrO_3^-$$

BrO_3^- is known to be a human carcinogen which can create anemia, cancer, vomiting, diarrhea, and central nervous system depression [3]. So, it is imperative to minimize the level of BrO_3^- to the permitted limit before being supplied for drinking purpose. Several methods have been executed to remove BrO_3^- from water samples but adsorption is extensively used due to easy operation, eco-friendly, and simple design [4–8]. Various types of adsorbents have been used for the removal of BrO_3^-, however, activated carbon (AC) is an efficient adsorbent due to its large surface area with surface functional groups and well developed porosity. AC can be prepared using any carbonaceous materials which have elemental carbon abundantly, however, coal and lignocellulosic materials are the two main sources for the development of ACs. Development of low cost AC is an important task. A low cost adsorbent is either abundantly available in nature or is a by-product waste material from industry. Recently, various agricultural waste materials have been used for the production of AC [9–17]. The carrot residue (CR), a fiber rich material, is available in large quantity during juice production. So, the target of the current study was to produce AC from CR and to assess environmental friendly BrO_3^- adsorption from water samples using CR-based AC. Batch studies were performed by changing various experimental conditions like pH, contact time, temperature, and

Correspondence: Dr. M. Naushad, Department of Chemistry, College of Science, Bld#5, King Saud University, Riyadh, Saudi Arabia
E-mail: shad81@rediffmail.com

Abbreviations: **AC**, activated carbon; **BET**, Brunauer–Emmett–Teller; **CAC**, carrot residue derived activated carbon; **CR**, carrot residue; **DTA**, differential thermal analysis; **EC**, European Commission; **EDX**, energy dispersive X-ray; **ESI**, electrospray ionization; **LOD**, limit of detection; **LOQ**, limit of quantification; **MRM**, multiple reaction monitoring; **RSD**, relative standard deviation; **SEM**, scanning electron microscopy; **TGA**, thermogravimetric analysis; **UPLC-MS**, ultra-performance liquid chromatography-mass spectrometry.

© 2016 WILEY-VCH Verlag GmbH & Co. KGaA, Weinheim

shaking speed. The analytical application of CAC was proven for the removal of BrO_3^- from tap and bottled water samples.

2 Material and methods

2.1 Reagents and materials

All chemicals and reagents used during this study were of analytical grade. CR was collected from vegetable area, Riyadh, Saudi Arabia.

2.2 Instrumentation and MS conditions

UPLC (Waters, Milford, MA, USA) was used to analyze BrO_3^- in water samples. The chromatographic separation of BrO_3^- was performed on a C_{18} column, $50 \times 2.1\ mm^2$ id and 1.7 μm particle size (Acquity BEH, Waters, Milford, MA, USA). The BrO_3^- optimal chromatographic separation was performed using water/formic acid, 99.9/0.1%, as a mobile phase. The mobile phase flow rate was $200\ \mu L\ min^{-1}$. The injection level of each sample was 5 μL.

The UPLC technique was interfaced with triple quadrupole mass spectrometer (MS/MS) (Micromass, Milford, MA, USA) which was equipped with an electrospray ionization (ESI) source. BrO_3^- detection was carried out in negative ionization mode and data acquisition was performed in the multiple reaction monitoring (MRM) mode. The most favorable ESI source working conditions were as follows: source temperature (120°C); capillary voltage (3 kV); desolvation temperature (350°C); cone voltage (30 V); cone gas flow rate ($60\ L\ h^{-1}$), and desolvation gas flow rate ($600\ L\ h^{-1}$). Cone gas (nitrogen) and collision gas (argon) were used of high purity. The applied UPLC-MS/MS method was previously developed [18]. The data acquisition was attained by Mass Lynx V4.1 software.

2.3 Quality parameters

The performance of the UPLC–MS system was assessed in terms of linearity, limit of detection (LOD, signal-to-noise ratio 3:1) and limit of quantification (LOQ, signal-to-noise ratio 10:1), and precisions (run-to-run and day-to-day). The linearity of the method was obtained by drawing calibration curves for peak area versus concentration ($0.005–10\ mg\ L^{-1}$). For the studied analyte the correlation coefficients (r^2) were >0.998. LOD and LOQ values were estimated by analyzing a blank sample (Milli-Q water, without BrO_3^-) spiked with BrO_3^-, $0.05\ mg\ L^{-1}$. LOD of $0.02\ mg\ L^{-1}$ and LOQ of $0.07\ mg\ L^{-1}$ were obtained. The run-to-run precision was calculated from five replicate BrO_3^- standard ($0.5\ mg\ L^{-1}$) injections on the same day. However, the day-to-day precision was estimated from five replicate BrO_3^- standard ($0.5\ mg\ L^{-1}$) injections over 3 successive days. The obtained relative standard deviation (RSD%) values for run-to-run precision and day-to-day precision were 1.63 and 2.13%, correspondingly. The achieved values showed that the applied method was precise which was essential for the accurate determination of BrO_3^- in water samples.

2.4 Preparation of CAC

CR was collected from a local fruit juice shop, Riyadh, Saudi Arabia. After the extraction of juice, the remaining lignocellulosic fiber was collected, washed with distilled water to remove impurities like dust from its surface, and then dried at 70°C in an oven for 24 h. The dried biomass was finally ground and treated with 1 M HNO_3 to remove soluble organic constituents and to introduce the new functional groups on the surface of raw CRs. After 24 h, the powder was filtered, washed with Milli-Q water five times and dried in an oven at 40°C. Thereafter, the HNO_3 treated powder was carbonized at 450°C in a horizontal tube furnace (id 65 mm, length 450 mm). The sample was kept in the reactor and heated at 450 ± 5°C for 1 h under nitrogen flow (flow rate $0.5\ L\ min^{-1}$). After the activation period, the sample was cooled down under nitrogen flow at room temperature and washed four to five times with Milli-Q water.

2.5 Characterization of CAC

The porous structure of the prepared CAC samples was determined using the Quantachrome surface area and pore size analyzer by N_2 adsorption at 77 K. Before the analysis, the sample was out-gassed at 100°C under vacuum for 12 h. The surface area and pore size distribution were evaluated using Brunauer–Emmett–Teller (BET) equation [19]. The total pore volume was evaluated by Barrett–Joyner–Halenda, BJH, method at P/Po 0.99 [20]. The FTIR absorption spectra of CAC and BCAC were recorded between 450 and $4000\ cm^{-1}$. The thermogravimetric analysis-differential thermal analysis (TGA-DTA) of CAC was taken at a heating rate of $10°C\ min^{-1}$ up to 1000°C in nitrogen atmosphere. The surface morphology and elemental composition of CAC and BCAC was performed using scanning electron microscopy with energy dispersive X-ray spectroscopy (SEM-EDX). The zero point charge (pH_{pzc}) was determined using 0.01 M NaCl at pH 2, 3, 5, 7, and 10. The pH values were adjusted using 0.1 M HCl/NaOH. 20 mg CAC was stirred for 24 h with 20 mL of 0.01 M NaCl solutions of different pH. After 24 h, the supernatant was poured and its final pH was measured. The value of pH_{pzc} was evaluated from a plot between pH_f and pH_i [21]. The functional groups on CAC were determined using the Boehm titration method using NaOH, Na_2CO_3 and $NaHCO_3$, and HCl as reagents [22]. Fifty milligram of CAC adsorbent was stirred with 50 mL of 0.05 M basic or acid solution in flasks for 24 h and then filtered. Thereafter, 10 mL of each solution was titrated with 0.05 M NaOH or HCl. According to the Boehm titration, $NaHCO_3$ can neutralize carboxyl groups, Na_2CO_3 can neutralize carboxyl, lactols, and lactones groups; and NaOH can neutralize carboxyl, lactols, lactones, and phenols groups [23].

2.6 Adsorption tests

Experiments were carried out by conventional batch method by agitating 50 mg CAC with 100 mL BrO_3^- solution of desired concentration ($1–50\ mg\ L^{-1}$), at initial pH 6.8 and constant temperature (25°C) in a water bath shaker at 150 rpm. After 1 h, the CAC sample was filtered off and the filtrate was analyzed for BrO_3^- concentration by UPLC-MS. All experiments were performed in triplicate and the average value was taken.

The amount of adsorbed BrO_3^- was calculated as:

$$q_e = \frac{(C_o - C_e)\ V}{m} \quad (1)$$

where C_e and C_o are the equilibrium and initial concentrations of BrO_3^- ($mg\ L^{-1}$), respectively, m is the mass of CAC (g), V is the volume of the BrO_3^- solution (L).

The kinetic, thermodynamic, and adsorption isotherm parameters for the adsorption BrO_3^- onto CAC were also done by batch studies.

© 2016 WILEY-VCH Verlag GmbH & Co. KGaA, Weinheim

CLEAN Soil Air Water

2.7 Analytical applications

Various samples of commercially available bottled water and tap water were collected for the analysis. In the drinking bottled water samples, the BrO_3^- concentration (<10 ng mL^{-1}) was given by the respective companies, and it was determined by UPLC-MS in the tap water samples. For the analysis, 50 mL of each water sample was taken in conical flask and shaken with 50 mg of CAC at optimum conditions (pH 3.5, temperature 40°C, and time 40 min). After 40 min, the concentration of BrO_3^- in each water sample was determined by UPLC-MS. Blanks and quality controls were analyzed in every batch to confirm that contamination of the samples did not occur and sensitivity of the detection was constant throughout the analysis.

3 Results and discussion

3.1 Characterization of CAC

On the basis of N_2 adsorption–desorption isotherms, the BET surface area, pore volume, and average pore diameter of CAC were 17.76 $m^2 g^{-1}$, 0.11 $cm^3 g^{-1}$, and 44.8 nm, respectively, and presented a type IV adsorption–desorption isotherm which is given by mesosporous materials [24]. The characteristic feature of type IV is its hysteresis loop. The hysteresis loop is associated with the secondary pore filling process of capillary condensation. To get the information about the surface functional groups and of adsorbent–adsorbate interactions, FTIR spectroscopy was used. Figure 1 shows the FTIR spectra of CAC and bromate adsorbed CAC (BCAC). The broad brands in the region of 3300 and 2925 cm^{-1} indicated the presence of surface

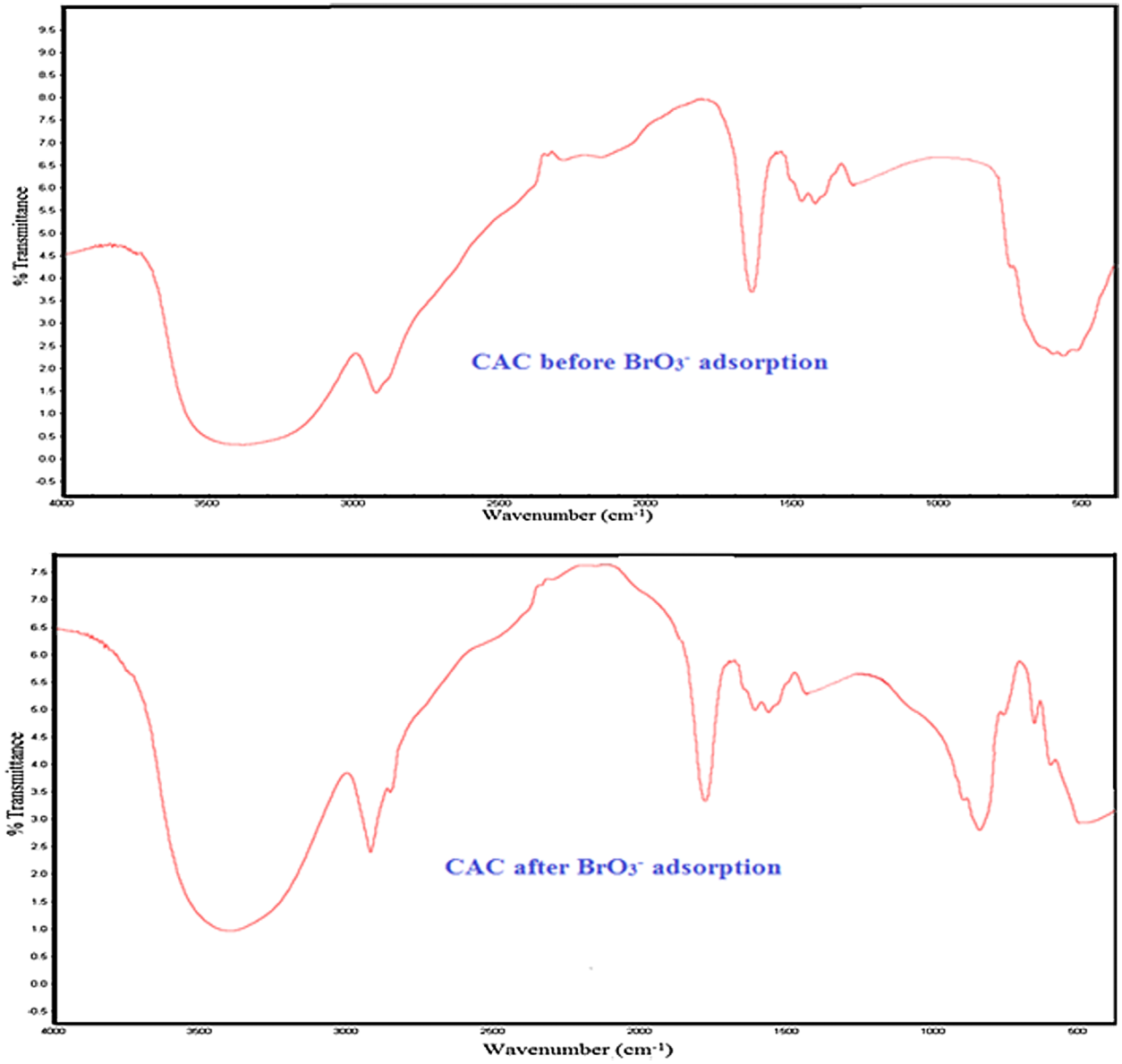

Figure 1. FTIR spectra of CAC before and after BrO_3^- adsorption.

hydroxyl (OH) and C–H groups, respectively [25, 26]. The peak at 1650 cm^{-1} was assigned to carbonyl groups. It was noted that the position as well as intensity of hydroxyl and carbonyl groups changed after the adsorption of BrO_3^- onto CAC which showed the participation of these groups in the adsorption process. A new Br–O peak appeared at 870 cm^{-1} which also showed the adsorption of bromate onto CAC. The study of the thermal degradation of materials is of major importance. The TGA-DTA of CAC (Fig. 2) showed 5.32% weight loss up to 200 °C which was due to the loss of external water molecules and volatile organic matters associated with the AC [27]. After that, a sharp weight loss (33.62%) between 200 and 400 °C was due to the decomposition of cellulosic material [28]. Beyond 400 °C, there was slow weight loss up to 800 °C, which might be due to the formation of carbon. The surface features of CAC and BCAC were studied by SEM. It can be seen from Fig. 3 that the CAC sample had a well-developed and uniform surface with an orderly pore structure. However, after BrO_3^- adsorption, the pores of CAC were covered by a white layer which showed the adsorption of BrO_3^- onto CAC. The EDX results also confirmed the adsorption of BrO_3^- onto CAC: before adsorption, the composition of CAC was 76.3% C, 8.5%, N, 6.2% O, 8.7% H, and 0.3% Ca. However, after adsorption it changed to 62.5% C, 4.8% N, 9.8% O, 17.5% Br, and 5.4% H.

The pH_{pzc} of CAC was found to be 4.2, which means that the surface of CAC was positively charged at $pH < 4.2$ and shows negative charge at $pH > 4.2$. On the basis of the Boehm tests, it was found that CAC had higher acidic groups which might be due to the treatment of CAC by HNO_3 which led to the acidic functional groups on the surface. CAC had 0.79 meq g^{-1} phenolic; 0.22 meq g^{-1} lactonic, and 0.14 meq g^{-1} carboxylic groups. So, the total acidic sites were 1.15 meq g^{-1}, while the basic sites were only 0.45 meq g^{-1}.

3.2 Removal of BrO_3^- by CAC

Figure 4a shows the percentage removal of BrO_3^- by CAC at different time. As given in Fig. 4a, the adsorption of BrO_3^- was rapid in the beginning and 63% BrO_3^- was adsorbed within 25 min. The equilibrium was achieved within 40 min with an adsorption rate of 93.7%. The fast adsorption of BrO_3^- at the beginning was might be due to the high availability of active sites at the surface on CAC. Since these sites were mostly occupied by BrO_3^- as well as the repulsion between the adsorbed BrO_3^- on the CAC surface and BrO_3^- in the solution phase, the adsorption rate decreased at the last. The solution pH is one of the crucial parameters which may change the degree of ionization of an adsorbate molecule and the surface charge of an adsorbent, thus affecting the adsorption capacity of an adsorbent [29–31]. The effect of pH for the removal of BrO_3^- by CAC was studied by performing equilibrium adsorption experiments at different pH values in the range of two to eight (Fig. 4b). In contrast, the other parameters like time, temperature, and initial concentration of BrO_3^- remained constant. Maximum adsorption (91%) was found in acidic medium in the pH range of 2–3.5 and thereafter, it started to decrease as the pH increased. At low pH, the higher adsorption of BrO_3^- was due to the significantly high electrostatic attraction between the positively changed surface of CAC and the negatively charged BrO_3^-. Beyond pH 4.2, the surface of CAC was negative, so the adsorption of BrO_3^- started to decrease. It was also reported by Xu et al. and Chen et al. that the optimum adsorption of BrO_3^- was in the pH range of 3–10 and 2, respectively [32, 33]. The results for the adsorption of BrO_3^- onto CAC with varying initial BrO_3^- concentrations (2–10 mg L^{-1}) at pH 3.5, CAC dosage 50 mg and contact time 40 min are given in Fig. 4c. The results showed that the adsorption removal efficiency was decreased by increasing the BrO_3^- concentration at fixed adsorbent dose. The higher adsorption of BrO_3^- at lower concentration was due to the presence of abundantly accessible active sites on the surface of CAC and the effective pore diffusivity decreased with increasing the initial BrO_3^- concentration [34]. The adsorptive removal of 5 mg L^{-1} BrO_3^- by CAC (50 mg/100 mL) at different temperatures (298, 303, 313, and 323 K) is shown in Fig. 4d. It was noted that 58.7% BrO_3^- was adsorbed at 298 K within 40 min. With increasing temperature from 298 to 313 K, the adsorption was also increased

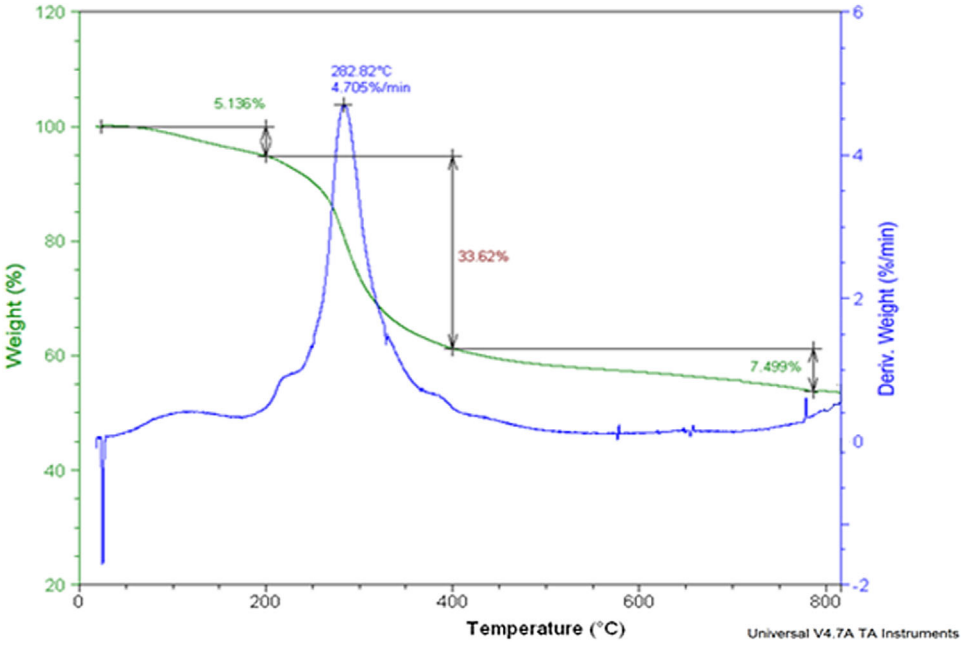

Figure 2. TGA-DTA curves of CAC.

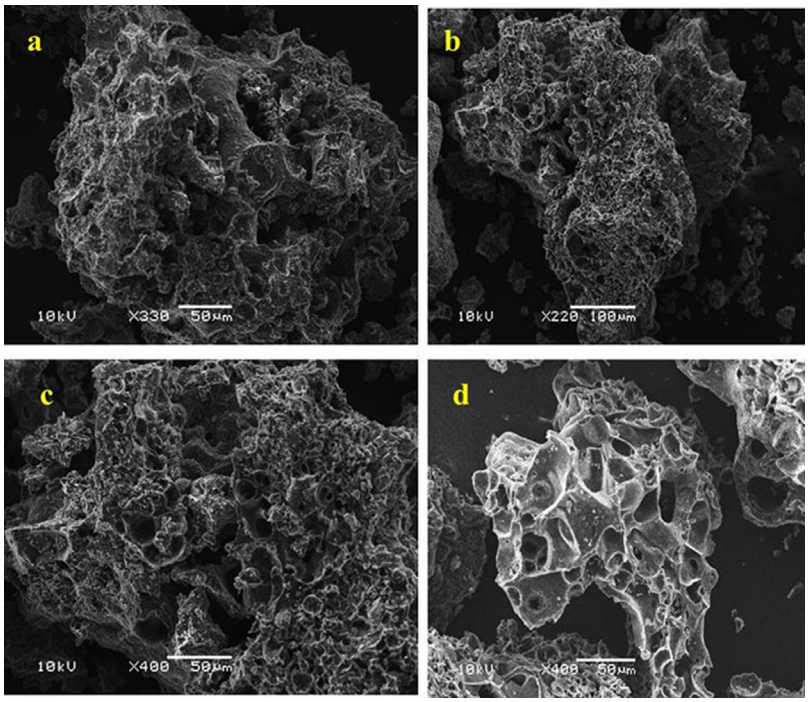

Figure 3. SEM images of CAC (a–c) before BrO_3^- adsorption at different magnifications, and (d) after BrO_3^- adsorption.

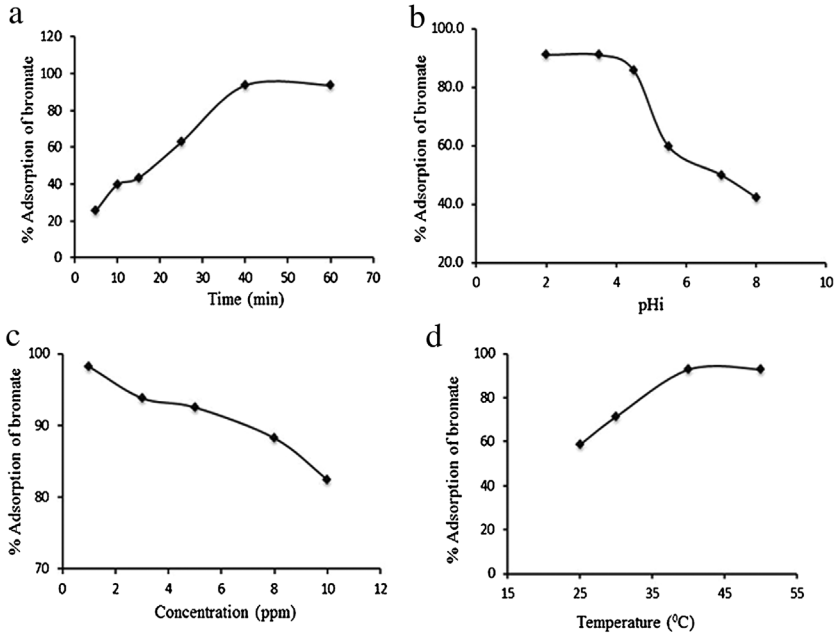

Figure 4. Effect of various operating parameters on the adsorption of BrO_3^- by CAC: (a) contact time, (b) pH_i, (c) initial concentration of BrO_3^-, and (d) temperature.

up to 92.8%. However, no change was noticed in the removal efficiency when the reaction temperature was raised from 313 to 323 K. The increase in BrO_3^- adsorption with temperature implies the adsorption process was more favorable at higher temperature and chemical in nature.

3.3 Desorption and regeneration studies

The regeneration of any adsorbents could prove double rewarding by stabilizing adsorbents and recovering valuable adsorbates, thereby decreasing demand for virgin adsorbents. In the present study, 0.1 M NaOH solution was used as an eluent for the desorption of BrO_3^-. The adsorption efficiency of regenerated CAC was checked four times and it was interesting to note that only 14.4% adsorption percentage was decreased after four consecutive cycles (Fig. 5). Therefore, CAC could be easily regenerated and used for the removal of BrO_3^- from water samples.

3.4 Kinetic studies

Kinetics can provide valuable understandings into reaction pathways and adsorption mechanisms. The kinetic data was fitted to

© 2016 WILEY-VCH Verlag GmbH & Co. KGaA, Weinheim

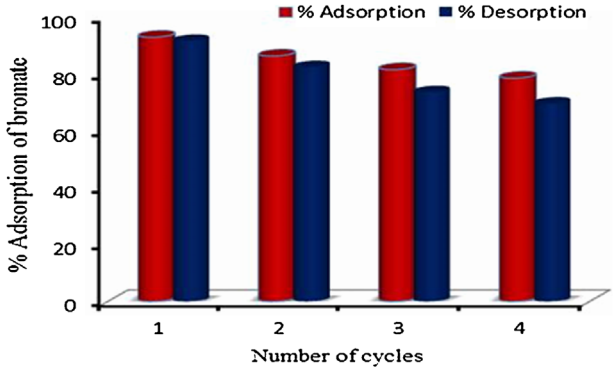

Figure 5. Regeneration studies for CAC (adsorbent dosage = 50 mg; equilibration time 40 min; volume 100 mL; initial concentration of BrO_3^- 5 mg L^{-1}; agitation speed 100 rpm).

pseudo-first-order and pseudo-second-order equations which are presented as [35, 36]:

Pseudo-first-order:

$$log\ (q_e - q_t) = log\ q_e - \frac{k_1\ t}{2.303} \tag{2}$$

Pseudo-second-order:

$$\frac{1}{q_t} = \frac{1}{k_2\ q_e^2} + \frac{1}{q_e} \tag{3}$$

where q_t and q_e are the amounts of BrO_3^- adsorbed at time t, and at equilibrium, respectively, k_1 (1 min^{-1}) and k_2 (g/mg min) are the rate constants for the pseudo-first-order and pseudo-second-order models, respectively. The values of k_1 and k_2 were evaluated from the slopes of the plots $log(q_e - q_t)$ versus t and t/q_t versus time, respectively (Fig. 6a and b). The results for these two models are given in Tab. 1. The high correlation coefficients (R^2) for pseudo-first-order model proved that the data obeyed well to the pseudo-first-order rate model which suggested that this model satisfactorily describe the adsorption of BrO_3^- onto CAC.

3.5 Adsorption isotherms

Langmuir and Freundlich adsorption isotherm models were studied (Fig. 6c and d).

The Langmuir isotherm model [37] can be represented as:

$$\frac{1}{q_e} = \frac{1}{q_m} + \frac{1}{b\ q_m\ C_e} \tag{4}$$

where C_e is the equilibrium residual BrO_3^- (mg L^{-1}), q_m (mg g^{-1}) is the maximum BrO_3^- adsorption capacity and b (L mg^{-1}) is the energy of adsorption. The values of q_m and b were calculated from the intercept and slope of linear plots of $1/q_e$ versus $1/C_e$, respectively (Tab. 2). The values of q_m increased with temperature which also confirmed the endothermic nature of BrO_3^- adsorption onto CAC.

A dimensionless equilibrium parameter (R_L) was evaluated as [38]:

$$R_L = \frac{1}{1 + b\ C_o} \tag{5}$$

where C_o is the lowest BrO_3^- initial concentration. The R_L value shows whether the adsorption is irreversible ($R_L = 0$), linear ($R_L = 1$), unfavorable ($R_L > 1$), or favorable ($0 < R_L < 1$). The values of R_L for the present study were found to be >0 and less than unity indicated the favorable adsorption of BrO_3^- onto CAC.

Freundlich isotherm [39] is given as:

$$log\ q_e = log\ K_f + \frac{1}{n} log\ C_e \tag{6}$$

where K_f (mg/g(L/mg)$^{1/n}$) and n (dimensionless) are the Freundlich isotherm constants. The values of n and K_f were evaluated from the slope ($1/n$) and intercept ($logK_f$) of the plot of $logq_e$ versus

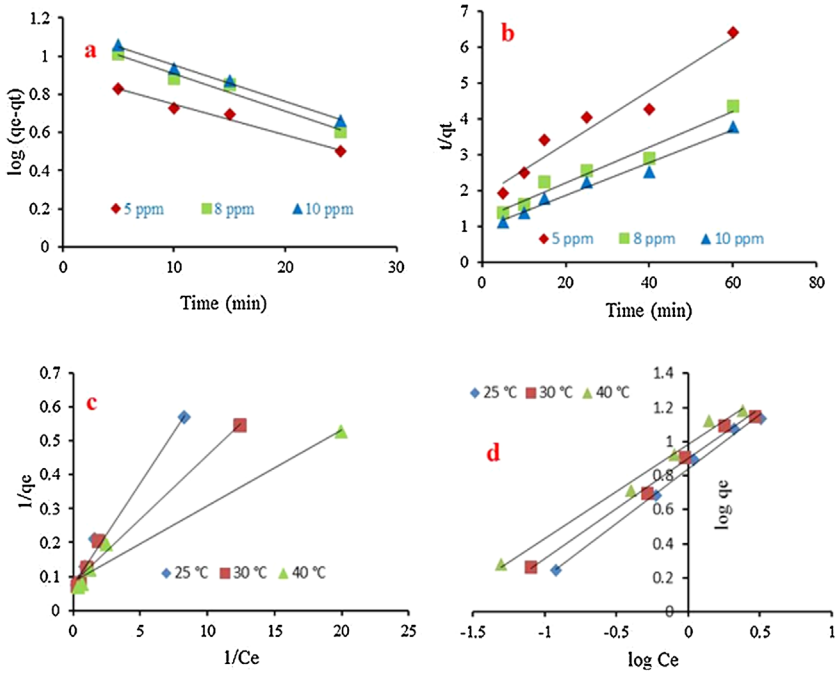

Figure 6. Plots of kinetic and isotherm models for the adsorption of BrO_3^- by CAC: (a) pseudo-first-order, (b) pseudo-second-order, (c) Langmuir isotherm, and (d) Freundlich isotherm models (agitation speed 100 rpm, adsorbent dosage = 50 mg; volume 100 mL; pH 3.5).

© 2016 WILEY-VCH Verlag GmbH & Co. KGaA, Weinheim

Table 1. Kinetic parameters for BrO_3^- adsorption using CAC

BrO_3^- initial concentration ($mg\,L^{-1}$)	Pseudo-first-order				Pseudo-second-order			
	Slope	Intercept	k_1 (min^{-1})	R^2	Slope	Intercept	k_2 ($g\,mg^{-1}\,min^{-1}$)	R^2
5	−0.016	0.91	3.68×10^{-2}	0.989	0.045	0.97	2.08×10^{-3}	0.974
8	−0.0197	4.53	4.53×10^{-2}	0.989	0.050	1.21	2.06×10^{-3}	0.962
10	−0.098	1.15	4.55×10^{-2}	0.992	0.073	1.85	2.88×10^{-3}	0.943

Table 2. Langmuir and Freundlich adsorption isotherm constants for the adsorption of BrO_3^- onto CAC

Temperature (°C)	Langmuir constant				Freundlich constant			
	q_m ($mg\,g^{-1}$)	b ($L\,mg^{-1}$)	R_L	R^2	$1/n$	n	K_f	R^2
25	16.66	0.83	0.19	0.988	0.642	1.55	6.91	0.995
30	27.03	0.46	0.30	0.978	0.588	1.70	7.94	0.991
40	45.46	0.26	0.43	0.971	0.556	1.79	9.66	0.992

Table 3. List of adsorbents available for the adsorption of BrO_3^-

Adsorbents	Experimental condition			Langmuir constant		Freundlich constant	
	Equilibration time (min)	Initial concentration of bromate ($mg\,L^{-1}$)	Temperature/ pH	b ($L\,mg^{-1}$)	q_m ($mg\,g^{-1}$)	n	K_f ($mg\,g^{-1}$) ($L\,mg^{-1}$)$^{1/n}$
De-Acidite FF-IP resin [42]	1	10	318/4–7	0.19	NA	NA	NA
Nano crystalline akaganeite coated quartz sand [32]	0.2	20	298/3–10	0.0456	5.09×10^{-4}	1.58	0.17
Granular ferric hydroxide(GFH) [43]	20	0.05	298/6–7	11.08	16.95	1.92	1.21
Amberlite IRA-400 [44]	0.5	40	293/6.5	1.99	0.57	1.53	1.74
DAC [26]	25	2	298/2–4	1.77	25.64	1.77	15.56
Organo-montmorillonite [45]	0.1	1440	298/6.3	0.089	NA	2	3.1
Nano-Al_2O_3 [46]	5.0	100	–	6.0	NA	NA	NA
CAC (present study)	40	5	313/3.5	0.26	45.46	1.79	9.66

NA, not available.

logC_e, respectively. The values of n were found to be >1 which indicated a good adsorption process [40]. Table 2 summarizes the values of Langmuir and Freundlich isotherm constants. It can be seen that the Freundlich model resulted into a better fit tha n the Langmuir model as the Freundlich isotherm model had higher values of correlation coefficients.

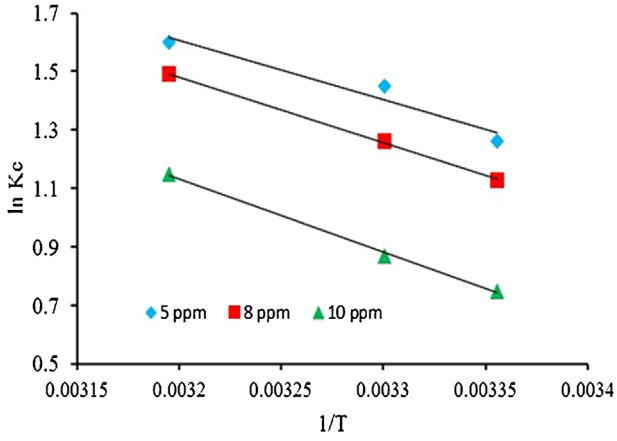

Figure 7. Van't Hoff plot for the adsorption of BrO_3^- onto CAC (adsorbent dosage = 50 mg; equilibration time 40 min; volume 100 mL; agitation speed 100 rpm).

3.6 Comparisons of adsorption capacity with other adsorbents

The adsorption capacity of the present adsorbent (CAC) which was determined from the Langmuir model was compared with the other adsorbents (Tab. 3) [26, 32, 41–46]. It is clear from Tab. 3 that the adsorption capacity of CAC for BrO_3^- was higher than

Table 4. Thermodynamics parameters for the adsorption of BrO_3^- onto CAC

C_o ($mg\,L^{-1}$)	ΔH^0 ($kJ\,mol^{-1}$)	ΔS^0 ($kJ\,mol^{-1}\,K^{-1}$)	$-\Delta G^0$ ($kJ\,mol^{-1}$)		
			298 K	303 K	313 K
5	16.81	0.067	3.17	3.51	4.18
8	18.54	0.071	2.81	3.17	3.89
10	20.86	0.076	1.84	2.23	2.98

© 2016 WILEY-VCH Verlag GmbH & Co. KGaA, Weinheim

Table 5. Amount of BrO_3^- in metropolitan and bottled water samples, before and after the adsorption onto CAC

Water sample	Water source	BrO_3^- (ng L^{-1}) ± SD	BrO_3^- amount provided on the label (ng L^{-1})
Sample 1[a)]	Desalinated water	52.37 ± 2.90	–
Sample 2[a)]	Desalinated water	38.46 ± 1.58	–
Sample 3[a)]	Desalinated water	65.32 ± 3.21	–
Sample 4[b)]	Well water	7.35 ± 0.10	<10
Sample 5[b)]	Well water	8.73 ± 0.11	<10
Sample 6[b)]	Well water	9.21 ± 0.13	<10

SD, standard deviation ($n = 3$); –, not described.
[a)] Metropolitan water had been pretreated with hypochlorite.
[b)] Bottled water underwent ozonation.

other adsorbents mentioned here as well as this adsorbent can be obtained cheaply in bulk quantity. Our findings showed the possible implications of CAC for BrO_3^- removal from water samples.

3.7 Thermodynamic studies

The thermodynamic parameters such as standard enthalpy change (ΔH^0), Gibb's free energy change (ΔG^0), and standard entropy change (ΔS^0) were evaluated using the following equations:

$$\Delta G^0 = \Delta H^0 - T\Delta S^0 \quad (7)$$

The values of ΔH^0 and ΔS^0 were determined from the slopes and intercepts of the van't Hoff plots (Fig. 7) given in Eq. (8).

$$\ln K_c = -\frac{\Delta H^0}{RT} + \frac{\Delta S^0}{R} \quad (8)$$

where K_c (L mg^{-1}) can be defined as:

$$K_c = \frac{C_{Ae}}{C_e} \quad (9)$$

where C_{Ae} (mg L^{-1}) and C_e (mg L^{-1}) are the equilibrium concentrations of adsorbate on solid and in solution phase, respectively.

The values of all three parameters are presented in Tab. 4. The positive values of ΔH^0 for all studied temperatures indicated the endothermic nature of the adsorption process. The negative values of ΔG^0 designated that the adsorption process was feasible and

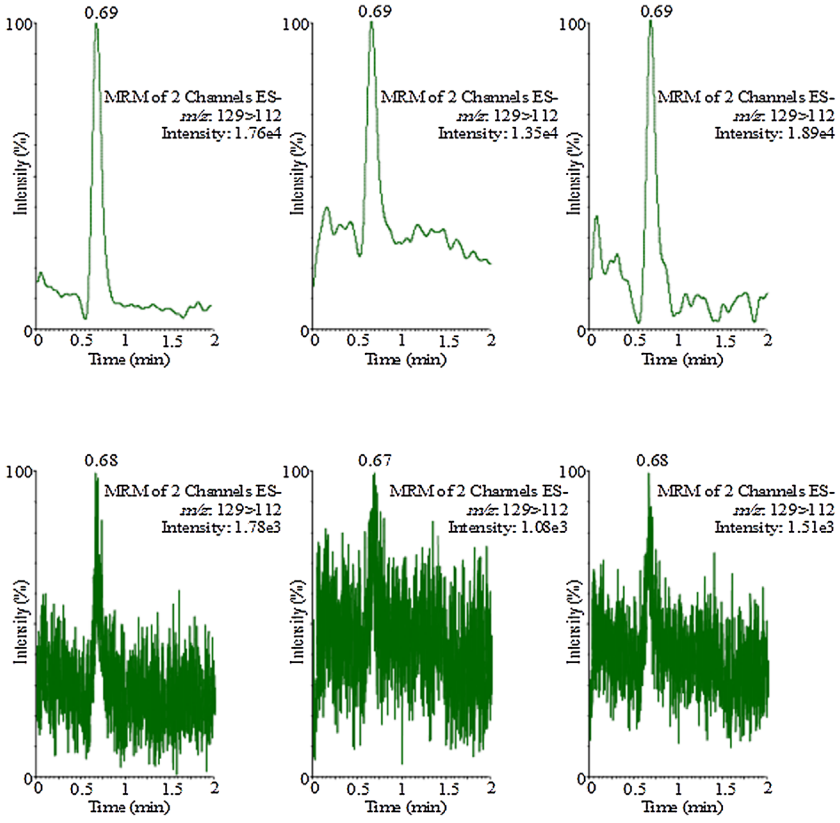

Figure 8. UPLC-MS chromatograms of BrO_3^- in three different metropolitan water samples before and after adsorption using CAC.

spontaneous in nature. The increase in ΔG^0 with temperature showed that the adsorption process was favorable at higher temperature. The positive values of ΔS^0 (disorder of the system) were observed which confirmed the increase in the randomness at the solid–solution interface.

3.8 Analysis of water samples

Table 5 summarizes the amounts of BrO_3^- found in metropolitan and bottled water samples, before and after the adsorption onto CAC. It is clear from the Tab. 5 that the concentration of BrO_3^- in all water samples was $<15\,ng\,L^{-1}$ before adsorption. But it was not detected after adsorption due to complete removal of BrO_3^- by CAC as can be seen form the chromatograms of BrO_3^- in the metropolitan water samples before and after adsorption (Fig. 8).

4 Concluding remarks

The present study showed that CAC was an economical, effective, and efficient bio-adsorbent for the removal BrO_3^- from water samples. Experimental parameters, such as contact time, initial concentration, pH, and temperature were optimized. A fast BrO_3^- adsorption with nearly 93.7% removal achieved within 40 min contacting time. The most suitable pH was found to be 3.5. The BrO_3^- adsorption onto CAC was well described by the Langmuir isotherm, however the kinetics corresponded to a pseudo-first-order equation. Overall, this study demonstrated that CAC derived from CR was a potential candidate for the removal of BrO_3^- from water samples, thus indicating a commendable substitute for the commercially available AC.

Acknowledgments

This project was funded by the National Plan for Science, Technology and Innovation (MAARIFAH), King Abdulaziz City for Science and Technology, Kingdom of Saudi Arabia (Award Number 12-WAT3138-02).

The authors have declared no conflicts of interest.

References

[1] WHO, *Guideline for Drinking-Water Quality*, Second addendum to 4th ed., WHO, Geneva **2011**.

[2] T. P. Bonacquisti, A Drinking Water Utility's Perspective on Bromide, Bromate, and Ozonation, *Toxicology* **2006**, *221*, 145–148.

[3] K. C. Campbell, Bromate-Induced Toxicity, *Toxicology* **2006**, *221*, 205–211.

[4] A. Bhatnagar, M. Sillanpää, Utilization of Agro-Industrial and Municipal Waste Materials as Potential Adsorbents for Water Treatment – A Review, *Chem. Eng. J.* **2010**, *168*, 493–504.

[5] M. Naushad, Z. A. ALOthman, G. Sharma, Inamuddin, Kinetics, Isotherm and Thermodynamic Investigations for the Adsorption of Co(II) Ion Onto Crystal Violet Modified Amberlite IR-120 Resin, *Ionics* **2015**, *21*, 1453–1459.

[6] D. Pathania, G. Sharma, A. Kumar, M. Naushad, S. Kalia, A. Sharma, Z. A. ALOthman, Combined Sorptional–Photocatalytic Remediation of Dyes by Polyaniline Zr(IV) Selenotungstophosphate Nanocomposite, *Toxicol. Environ. Chem.* **2015**, *97*, 526–537.

[7] M. Naushad, Z. A. ALOthman, M. M. Alam, M. R. Awual, G. E. Eldesoky, M. Islam, Synthesis of Sodium Dodecyl Sulfate-Supported Nanocomposite Cation Exchanger: Removal and Recovery of Cu^{2+} from Synthetic, Pharmaceutical and Alloy Samples, *Iran. J. Chem.* **2015**, *12*, 1677–1686.

[8] S. M. Alshehri, M. Naushad, T. Ahamad, Z. A. Alothman, A. Aldalbahi, Synthesis, Characterization of Curcumin Based Ecofriendly Antimicrobial Bio-Adsorbent for the Removal of Phenol from Aqueous Medium, *Chem. Eng. J.* **2014**, *254*, 181–189.

[9] V. Gomez-Serranoa, P. M. A. lvarezb, J. Jaramilloa, F. J. Beltran, Formation of Oxygen Structures by Ozonation of Carbonaceous Materials Prepared from Cherry Stones: II. Kinetic Study, *Carbon* **2002**, *40*, 523–529.

[10] M. L. Martinez, M. M. Torres, C. A. Guzman, D. M. Maestri, Preparation and Characteristics of Activated Carbon from Olive Stones and Walnut Shells, *Ind. Crops Prod.* **2006**, *23*, 23–28.

[11] C. Sentorun-Shalaby, M. G. Ucak-Astarlioglu, L. Artok, C. Sarici, Preparation and Characterization of Activated Carbons by One-Step Steam Pyrolysis/Activation from Apricot Stones, *Microporous Mesoporous Mater.* **2006**, *88*, 126–134.

[12] R. V. R. A. Rios, M. Martinez-Escandell, M. Molina-Sabio, F. Rodriguez-Reinoso, Carbon Foam Prepared by Pyrolysis of Olive Stones Under Steam, *Carbon* **2006**, *44*, 1448–1454.

[13] N. M. Haimour, S. Emeish, Utilization of Date Stones for Production of Activated Carbon Using Phosphoric Acid, *Waste Manage.* **2006**, *26*, 651–660.

[14] Z. Merzougui, F. Addoun, Effect of Oxidant Treatment of Date Pit Activated Carbons Application to the Treatment of Waters, *Desalination* **2008**, *222*, 394–403.

[15] C. A. Toles, W. E. Marshall, M. M. Johns, L. H. Wartelle, A. McAloon, Acid-Activated Carbons from Almond Shells: Physical, Chemical and Adsorptive Properties and Estimated Cost of Production, *Bioresour. Technol.* **2000**, *71*, 87–92.

[16] C. Erlich, E. Bjornbom, D. Bolado, M. Giner, T. H. Fransson, Pyrolysis and Gasification of Pellets from Sugar Cane Bagasse and Wood, *Fuel* **2006**, *85*, 1535–1540.

[17] K. L. Wasewar, P. Kumar, S. Chand, B. N. Padmini, T. T. Teng, Adsorption of Cadmium Ions from Aqueous Solution Using Granular Activated Carbon and Activated Clay, *Clean – Soil Air Water* **2010**, *38*, 649–656.

[18] I. H. Alsohaimi, Z. A. Alothman, M. A. Abdalla, A. K. Alomary, R. Busquets, M. R. Khan, Determination of Bromate in Drinking Water by Ultra-Performance Liquid Chromatography-Tandem Mass Spectrometry, *J. Sep. Sci.* **2012**, *35*, 2538–2543.

[19] S. Brunauer, P. Emmett, E. Teller, Adsorption of Gases in Multimolecular Layers, *J. Am. Chem. Soc.* **1938**, *60*, 309–319.

[20] E. P. Barrett, L. C. Joyner, P. H. Halenda, The Determination of Pore Volume and Area Distribution in Porous Substances, *J. Am. Chem. Soc.* **1951**, *73*, 373–380.

[21] B. Petrova, T. Budinova, B. Tsyntsarski, V. Kochkodan, Z. Shkavro, N. Petrov, Removal of Aromatic Hydrocarbons from Water by Activated Carbon from Apricot Stones, *Chem. Eng. J.* **2010**, *165*, 258–264.

[22] H. P. Boehm, Some Aspects of the Surface Chemistry of Carbon Blacks and Other Carbons, *Carbon* **1994**, *32*, 759–764.

[23] F. Guzel, H. Yakut, G. Topal, Determination of Kinetic and Equilibrium Parameters of the Batch Adsorption of Mn(II), Co(II), Ni(II) and Cu(II) from Aqueous Solution by Black Carrot (*Daucus carota* L.) Residues, *J. Hazard. Mater.* **2008**, *153*, 1275–1287.

[24] T. K. Saha, N. C. Bhoumik, S. Karmaker, M. G. Ahmed, H. Ichikawa, Y. Fukumori, Adsorption Characteristics of Reactive Black 5 from Aqueous Solution onto Chitosan, *Clean – Soil Air Water* **2011**, *39*, 984–993.

[25] M. Naushad, Z. A. ALOthman, H. Javadian, Removal of Pb(II) from Aqueous Solution Using Ethylene Diamine Tetra Acetic Acid–Zr(IV) Iodate Composite Cation Exchanger: Kinetics, Isotherms and Thermodynamic Studies, *J. Ind. Eng. Chem.* **2015**, *25*, 35–41.

[26] A. Alqadmi, M. Naushad, T. Ahamd, M. A. Abdalla, Z. A. ALOthman, S. M. AlShehri, Synthesis and Characterization of Fe_3O_4@TSC Nanocomposite: Highly Efficient Removal of Toxic Metal Ions from Aqueous Medium, *RSC Adv.* **2016**, *6*, 22679–22689.

© 2016 WILEY-VCH Verlag GmbH & Co. KGaA, Weinheim

[27] M. Naushad, Z. A. ALOthman, M. R. Awual, M. M. Alam, G. E. Eldesoky, Adsorption Kinetics, Isotherms, and Thermodynamic Studies for the Adsorption of Pb^{2+} and Hg^{2+} Metal Ions from Aqueous Medium Using Ti(IV) Iodovanadate Cation exchanger, *Ionics* **2015**, *21*, 2237–2245.

[28] M. Naushad, M. R. Khan, Z. A. ALOthman, I. AlSohaimi, F. Rodriguez-Reinoso, M. Turki, R. Ali, Removal of BrO_3− from Drinking Water Samples Using Newly Developed Agricultural Waste-Based Activated Carbon and Its Determination by Ultra-Performance Liquid Chromatography-Mass Spectrometry, *Environ. Sci. Pollut. Res*. **2015**, *2*, 15853–15865.

[29] B. K. Nandi, A. Goswami, M. K. Purkait, Adsorption Characteristics of Brilliant Green Dye on Kaolin, *J. Hazard. Mater*. **2009**, *161*, 387–395.

[30] Z. A. ALOthman, M. Naushad, R. Ali, Kinetic, Equilibrium Isotherm and Thermodynamic Studies of Cr(VI) Adsorption onto Low-Cost Adsorbent Developed from Peanut Shell Activated with Phosphoric Acid, *Environ. Sci. Pollut. Res*. **2013**, *20*, 3351–3365.

[31] A. Kumar, G. Sharma, M. Naushad, P. Singh, S. Kalia, Polyacrylamide/Ni0.02Zn0.98O Nanocomposite with High Solar Light Photocatalytic Activity and Efficient Adsorption Capacity for Toxic Dye Removal, *Ind. Eng. Chem. Res*. **2014**, *53*, 15549–15560.

[32] C. Xu, J. Shi, W. Zhou, B. Gao, Q. Yue, X. Wang, Bromate Removal from Aqueous Solutions by Nano Crystalline Akaganeite (β-FeOOH)-Coated Quartz Sand (CACQS), *Chem. Eng. J*. **2012**, *187*, 63–68.

[33] H. Chen, Z. Xu, H. Wan, J. Zheng, D. Yin, S. Zheng, Aqueous Bromate Reduction by Catalytic Hydrogenation over Pd/Al_2O_3 Catalysts, *Appl. Catal., B* **2010**, *96*, 307–313.

[34] G. Skodras, I. Diamantopoulou, G. Pantoleontos, G. P. Sakellaropoulos, Kinetic Studies of Elemental Mercury Adsorption in Activated Carbon Fixed Bed Reactor, *J. Hazard. Mater*. **2008**, *158*, 1–13.

[35] S. Lagergren, About the Theory of So Called Adsorption of Soluble Substances, Kungliga Svenska Vetenskapsakademiens, *Handlingar* **1898**, *24*, 1–39.

[36] Y. S. Ho, G. McKay, Sorption of Dye from Aqueous Solution by Peat, *Chem. Eng. J*. **1998**, *70*, 115–124.

[37] I. Langmuir, The Adsorption of Gases on Plane Surfaces of Glass, Mica and Platinum, *J. Am. Chem. Soc*. **1918**, *40*, 1361–1403.

[38] R. Bushra, M. Naushad, R. Adnan, Z. A. ALOthman, M. Rafatullah, Polyaniline Supported Nanocomposite Cation Exchanger: Synthesis, Characterization and Applications for the Efficient Removal of Pb^{2+} Ion from Aqueous Medium, *J. Ind. Eng. Chem*. **2015**, *21*, 1112–1118.

[39] H. M. F. Freundlich, Over the Adsorption in Solution, *J. Phys. Chem*. **1906**, *57*, 385–470.

[40] C. Namasivayam, R. T. Yamura, D. J. S. E. Arasi, Removal of Acid Violet from Wastewater by Adsorption on Waste Red Mud, *Environ. Geol*. **2001**, *41*, 269–273.

[41] P. Mondal, B. Mohanty, C. B. Majumde, Removal of Arsenic from Simulated Groundwater Using GAC-Ca in Batch Reactor: Kinetics and Equilibrium Studies, *Clean – Soil Air Water* **2012**, *40*, 506–514.

[42] M. Naushad, Z. A. ALOthman, M. R. Khan, S. M. Wabaidur, Removal of Bromate from Water Using De-Acidite FF-IP Resin and Determination by Ultra-Performance Liquid Chromatography-Tandem Mass Spectrometry, *Clean – Soil Air Water* **2013**, *41*, 528–533.

[43] A. Bhatnagara, Y. H. Choi, Y. J. Yoon, Y. Shin, B. H. Jeon, J. W. Kang, Bromate Removal from Water by Granular Ferric Hydroxide (GFH), *J. Hazard. Mater*. **2009**, *170*, 134–140.

[44] M. Naushad, M. R. Khan, Z. A. ALOthman, M. R. Awual, Bromate Removal from Water Samples Using Strongly Basic Anion Exchange Resin Amberlite IRA-400: Kinetics, Isotherms and Thermodynamic Studies, *Desalin. Water Treat*. **2016**, *57*, 5781–5788.

[45] R. Chitrakar, Y. Makita, A. Sonoda, T. Hirotsu, Adsorption of Trace Levels of Bromate from Aqueous Solution by Organo-Montmorillonite, *Appl. Clay Sci*. **2011**, *51*, 375–379.

[46] A. Bhatnagar, M. Sillanpää, Sorption Studies of Bromate Removal from Water by Nano-Al_2O_3, *Sep. Sci. Technol*. **2012**, *47*, 89–95.

© 2016 WILEY-VCH Verlag GmbH & Co. KGaA, Weinheim